Real-time surface defect detection and the traceable measurement of defect depth in 3D

M. Tailor, P. Phaithoonbuathong, J. Petzing, M. Jackson, R. Parkin
EPSRC Centre for Innovative Manufacturing in Intelligent Automation,
Wolfson School of Mechanical & Manufacturing Engineering,
Loughborough University, UK
Corresponding Individual: m.tailor@lboro.ac.uk

Abstract

Three-dimensional non-contact optical surface topography and coordinate geometry measurement are of significant interest to many industrial sectors. The current requirement is to speed up inspection processes, increase sensor resolution, and sensor accuracy. This is not necessarily the case for online surface defect inspection. Human visual analysis of surface defects (pits, scratches, etc) is qualitative and subjective. Automated non-contact analysis should provide a robust and systematic quantitative route for defect assessment. However, different optical transducers use disparate physical principles, interact with surfaces and defects in diverse ways, leading to variation in measurement data from one instrument to the next. Instrument "black box" software is often non-traceable, leading to significant uncertainty about data manipulation. This is compounded by a lack of traceable surface defect standards and defect soft gauges with which to test the instruments and software respectively.

This work reports the development of novel traceable surface defect artefacts (typically 100 μm wide by 10 μm deep) produced using Vickers equipment on flat metal plates with varying scales of surface roughness, and the development of a novel traceable, repeatable, mathematical solution for automatic defect detection and absolute depth measurement. Comparative results show that the new surface defect detection/quantification is more efficient, repeatable and robust than alternative measurement processes using a range of instrumentation based (and third party) software solutions.

1 Introduction

Inspection of surface defects has become a critical task for manufacturers who strive to improve product quality and production efficiency. Non-contact optical measurement methods for surface defect analysis in three dimensions (3D) is increasing in industrial popularity, with demands to speed up, increase the resolution, and improve the accuracy of the inspection process, thus improving manufacturing quality. Many manufacturing processes have become fully automated resulting in high production volumes. However, this is not necessarily the case for the inspection of surface imperfections.

The automated detection of process-induced defects such as pits, scratches and dinks is a common and important problem in machine vision, on substrates ranging across many different industrial sectors, including automotive, aerospace, optics and electronics with examples in literature discussing the detection of 2D and 3D defects in various applications. Examples include; the robust and efficient automated detection of tooling defects [1] for polished stone, computer-aided visual inspection system for surface defect detection in ceramic capacitor chips [2], the real time defect detection on highly reflected curved surfaces [3], along with vision inspection systems for surface defects on high reflective metal substrates [4].

Once potential defects have been identified, it is very important to extract the defect accurately from the surface, obtained either from the 2D or 3D surface topography measurement system. Tsai *et al* have developed several algorithms for precise defect detection in images from different applications [5-8]. A wavelet analysis approach has also been implemented for detecting defects [9]. Once detected, it then becomes important to quantify the defect geometry (such as depth) in response to quality-assurance and functional specifications. Although significant work has been completed in detecting surface defects using a variety of instrument solutions, robust, traceable and automatic methods for depth quantification of 3D defects is less well explored.

Currently, standards based on the ISO Geometrical Product Specification (GPS) are available to quantify surface features in terms of roughness parameters from contact and non-contact surface profilometry (such as *Rp*, *Rv* and *Rz*), which have been adopted to measure the amplitude characterstics of defects from a traditional surface metrology perspective [10-12]. These standards provide tools to allow the measurement of negative or positive height components with respect to least squares mean line datums or planes fitted through the surface profiles, and also material probability curves (the Abbott Curve). But these standards focus on surface topography (typically high frequency / small wavelength features) but do not uniquely isolate larger scale defects and correctly measure the depth of such defects.

In this research, a novel algorithm is being developed for measuring the depth of the surface defect automatically. The artefact generation, novel algorithm and comparative results between manual and automatic depth measurement are presented.

2 Artefact Generation

There is little evidence of standard, traceable, surface defect comparators commercially available and hence there is a need to generate standard surface defect artefacts. In this context, the term traceable means that the geometric parameters of a standard defect (depth for instance) can be directly traced to the SI definition of the metre. In this research, artefacts have been generated using repeatable Vickers hardness testing equipment, more typically used to determine the hardness of a substrate. Indentations are made using a known pyramidal indenter that creates a dent on the metal surface. Irrespective of the material hardness, this indentation has a very unique shape and geometry that can be used as a standard defect to develop the measurement method for finding the depth of the defect.

By varying the load, four different sizes of indentation have been embedded into flat standard stainless steel following the specifications set out in BS EN ISO 6507-1 [13], these nominally being 10 µm, 20 µm, 30 µm, and 45 µm deep. Similar sets of indentations have been produced on four stainless steel plates having different surface roughness values. The measured *Rq* values of the four stainless steel substrates [10] is 0.06 µm, 0.16 µm, 0.78 µm and 1.27 µm respectively, when using a Taylor Hobson Form Talysurf Intra to generate 2D line profiles. An example of one particular defect is shown in Figure 1.

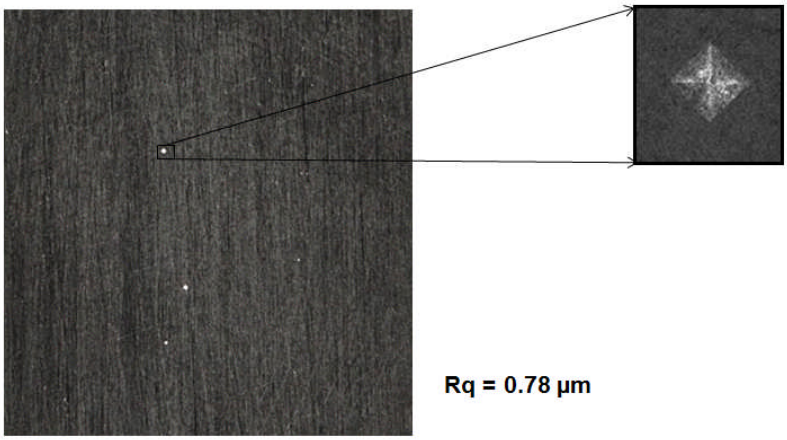

Figure 1: Pyramidal artefacts in a stainless steel substrate

2.1 3D Data Acquisition

The indentations have been measured using a Zygo NewView 5000 coherence scanning interferometer, that was traceably calibrated with reference to NIST certified calibration artefacts. The Zygo is a 3D optical sensor based on scanning white light interferometry technology and is capable of measuring a variety of surface types, including ground and polished surfaces, steps and films.

For measuring the artefacts, a 10x Mirau objective lens was selected with 1x optical zoom, producing 3D datasets with a field of view of approximately 0.7 mm x 0.53 mm.

2.2 Manual Depth Measurement

The first analysis of the defect data was completed on a manual basis to illustrate typical current capability. This means that third party software tools were used to process (as much as possible) the defect, and quantify the geometry of the defects. Once the 3D data was acquired from the Zygo, it was processed using DigitalSurf MountainsMap (v5) software. Due to the limitations of the initial measuring equipment, the datasets often contained non-measured data points (holes or voids) that required filling. This was achieved using the MountainsMap software's built-in linear interpolation toolbox.

Typically, the 3D datasets also contained geometric form that needed to be removed for better assessment of the surface. Leaving large scale form in place would often mask the defect detail. Once the form was removed through least squares techniques, it was possible to generate a cross sectional profile at the users perceived deepest point of each defect, allowing the manual measurement the depth of the defect. The profile height parameter *Pt* was used to measure the depth charateristics of each defect, where *Pt* is defined as [10],

"Total height of the profile Pt is a sum of the height of the largest profile peak height Pp and the largest profile valley depth Pv within the evaluation length"

This process is illustrated in Figure 2, showing the 3D defect on a smooth substrate as a greyscale plot, with a line profile created through the maximum point of defect depth. The subsequent *Pt* value of 44.8 µm is illustrated on the line profile although clearly the analysis is subjetive in terms of the operator defining the orientation and position of the line profile and it should not be underestimated how long this process can take when a surface defect is masked by significant surface roughness. It should also be noted that the use of the *P* parameter analysis does not include any further band pass filtering of the surface data (into roughness or waviness components) although in this example it is not necessary due to the smooth nature of the substrate.

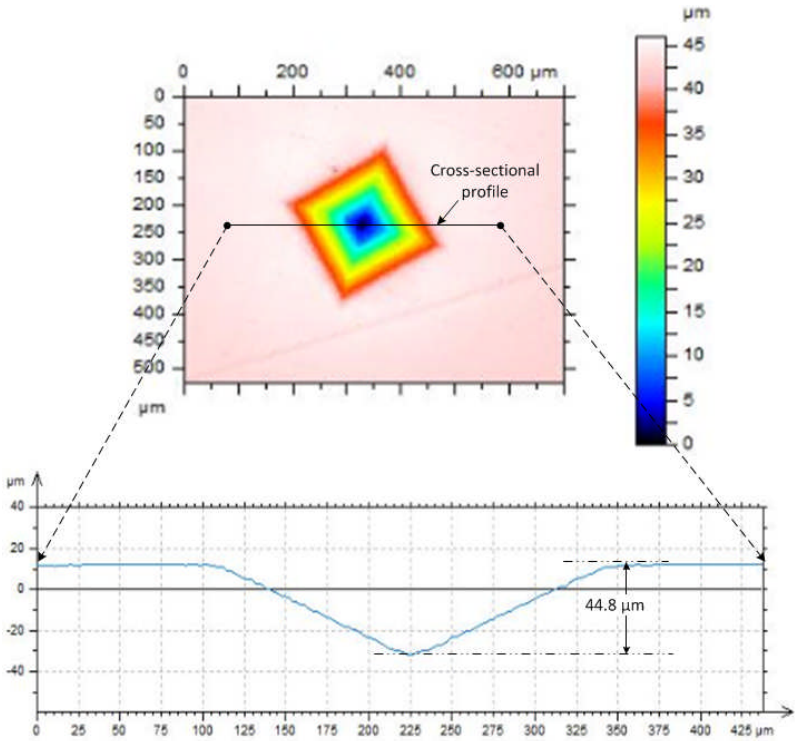

Figure 2 : Manual depth measurement method on a smooth substrate defect

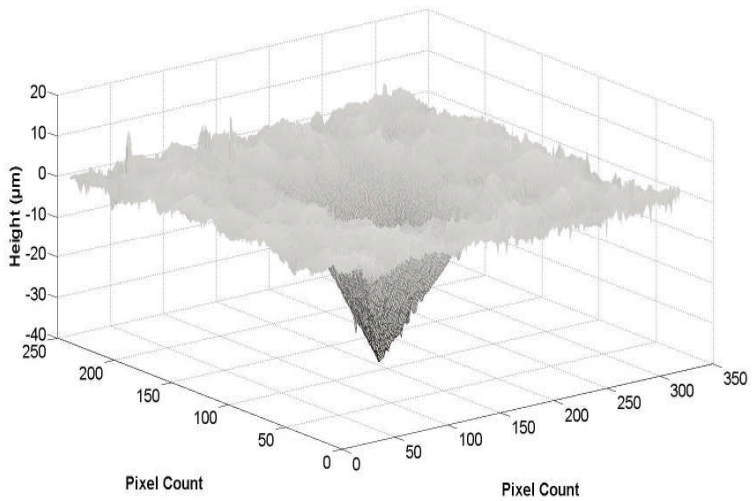

Figure 3 : Defect embedded in a substrate exhibiting significant roughness

3 Novel Algorithm

The novel defect processing algorithm reported here has been developed using MATLAB R2011b and is briefly illustrated in Figure 4. The Zygo provides 3D point cloud data as the output of the measured surface. As explained earlier in Section 2.2 it is essential to fill the non-measured data points and remove the form from the surface. To process this point cloud data in MATLAB it is necessary to convert the Zygo's native format into text format, this being achieved using the MountainMaps software. Figure 3 shows noisy 3D data of a measured surface (Rq = 0.78 µm) with geometric form removed. Note that due to constraints of the Matlab processing and the aspect ratio of the defect, the height data is given in micrometres, but the X and Y ordinates are provided as a pixel count. Given that the field of view is several hundred micrometres on a side, if the dataset was shown with the X and Y ordinates in micrometres, very little detail of the defect would be seen due to its relatively shallow depth.

Instrument noise and measurement noise is always present in acquired data from any 3D measurement instrument and it is again important to remove the noise for accurate depth measurement. If this is not completed, then spurious peaks within the data could lead to incorrect depth measurement. A one dimensional Gaussian filter was designed to remove the noise from the surface data. Once the noise was removed it was important to seperate the defect from the surface. The purpose of this process is to outline the region of interest and 3D data portions for later dimensional calculations. In human-visual inspection, the defect boundary is defined as the change of surface height on the 3D data. There are a number of image processing/mathematical techniques available such as Edge detection using gradient operators, and thresholding, to be used for the segmenting of the defective region from the background. Due to the embedded surface roughness, edge detection using gradient operators was found to be too complex and hence thresholding methods were implemented to define the defect region.

Once the defect region was seperated using the thresholding method, it was relatively straight forward to derive the boundary of the defect region in 3D that can be seen as a black circumferential line at the throat of the defect in Figure 5. This allows a least square plane to be fitted into the detected defect boundary data points. In a measured field of view, the algorithm tries to find the point that has minimum value in the Z direction which is ultimately the deepest point of the defect. The perpendicular distance from the deepest point to the generated least square plane is effectively the depth of the defect. This process was applied to the range of substrates and depths of defect identified in Section 2.0, and the results of the automatic analysis are discussed below.

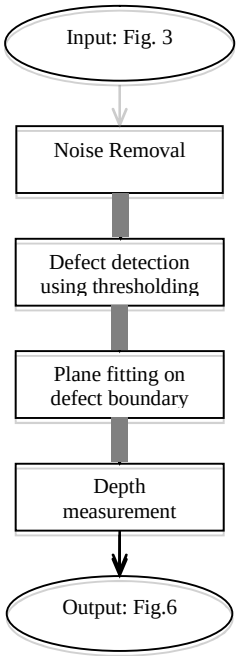

Figure 4 : Flowchart of the novel depth measurement method

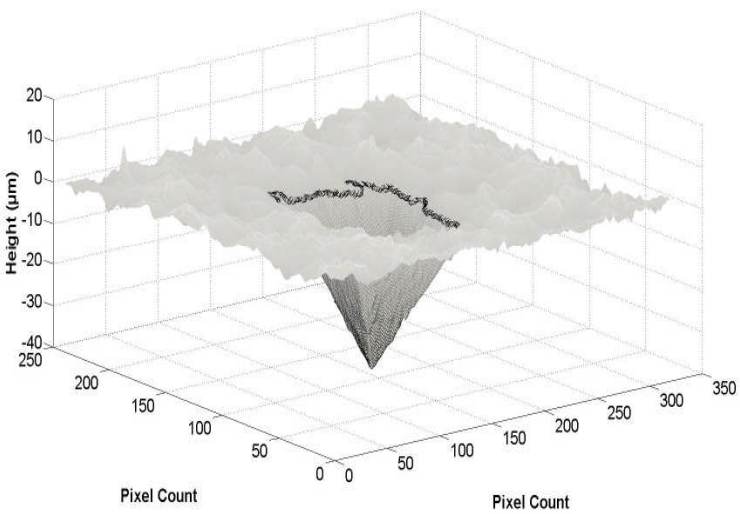

Figure 5 : Highlighted defect boundary of the data shown in Figure 3

4 Results and Discussions

The comparative analysis of manual defect assessment and automatic defect assessment using the new algorithm is shown in Figure 6. In this example four defects are measured on the 0.78 µm (*Rq*) stainless steel sample. In each case the manual height measurement (repeated five times for each defect) consistently reports a larger depth value than the corresponding automated process, although this difference decreases from the deepest defect to the shallowest defect. Furthermore, the variability of the manual measurement process (illustrated by the one sigma standard deviation error bars) is also larger than that for the automated process. Both of these differences are a function of the subjectivity of profile selection by the user when completing the manual measurements. It should be noted that each manual defect measurement typically takes a few minutes to complete, whereas the automated process takes just a few seconds.

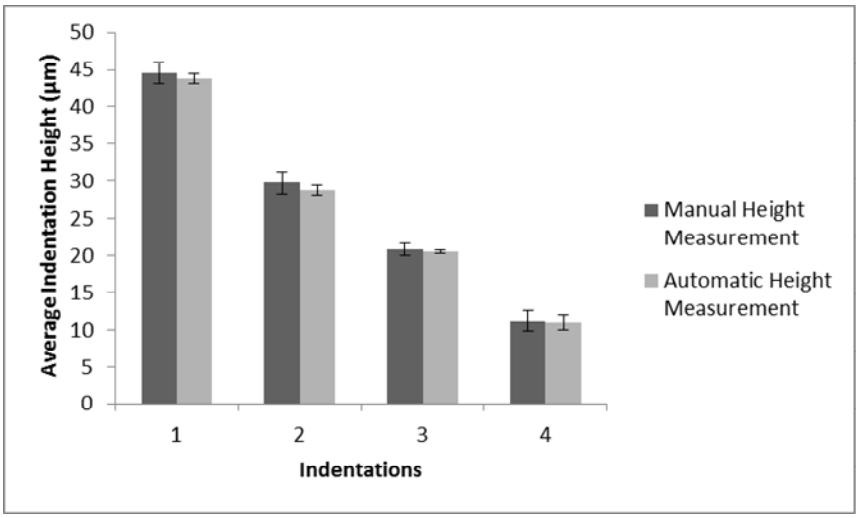

Figure 6: Comparative analysis of manual and automated defect processing

A key element of this work is to be able to identify how effective the developed automated process is when dealing with defects embedded in substrates exhibiting a range of surface roughness. Figure 7 shows a comparison of the manual and automated measurement of the nominal 30 µm deep defects in the four substrates of increasing surface roughness, from 0.06 µm to 1.27 µm *Rq* respectively.

The trend is for the manual and automatic assessments to be initailly well correlated, but as the surface roughness increases, the correlation deteriorates. In smooth substrates, there is clear definition of the boundaries of the indented defect, consequently the two measurement approaches can clearly define the defect boundary conditions. As the surface roughness increases, then defining the defect boundary becomes more problematic, with spurious surface peaks and valleys disrupting the boundary conditions. Consequently both measurement

approaches tend to underestimate the defect geometry for samples with higher surface roughness.

The new automated algorithm processes the data efficiently for all four cases, but the boundary definition of the defect is seen to be deeper into the defect throat for rougher substrates (as illustrated in Figure 5 – black circumferential line inside the defect). This is because the software is establishing an initial continuous boundary condition for the defect, before calculating geometric parameters. It is fully anticipated that if the substrate surface roughness is too large, then visually identifying defects will become more problematic, and automatically calculating the geometric parameters will be more prone to uncertainty. The results presented in Figure 7 suggest that any measurement (manual or automated) will underestimate defect geometry (in this case defect depth) in surfaces with roughness averages of more than 1.0 µm *Rq*.

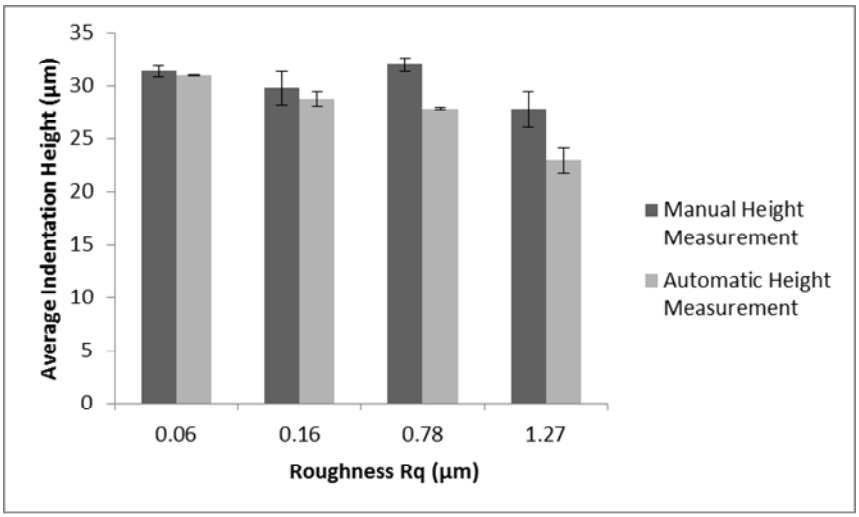

Figure 7: Influence of substrate surface roughness on manual and automated defect processing

5 Conclusion

The current research has identified the need for improving the capability and efficacy of three dimensional surface defect detection and characterization in a range of applications. This has been hampered by an apparaent lack of commercially traceable defect standards, from which comparative development of new mathematical solutions can be completed, and limitations to existing software tools used for defect quantification. To date, this research has developed and successfully demonstrated:

- Traceable and repeatable defect generation in a range of substrates with varying roughness and definitions of surface roughness limits.

- Rapid, automated measurement of defects using a new Matlab based suite of algorithms, with a high level of repeatability on the defect depth measurement.

This work is currently being extended to evaluate defect area, volume and shape, with full details of these measurements and the mathematical background of the image processing, to be published in the near future.

References

[1] Lee J, Smith M, Smith L, Midha P, Robust and efficient automated detection of tooling defects in polished stone, Comput. Ind., 56(8),787-801, 2005.
[2] Lin H, Computer-aided visual inspection of surface defects in ceramic capacitor chips, J. Mater. Process Technol., 189(1), 19-25, 2007.
[3] Rosati G, Boschetti G, Biondi A, Rossi A, Real-time defect detection on highly reflective curved surfaces, Opt. Las. Eng., 47(3), 379-384, 2009.
[4] Xue-wu Z, Yan-qiong D, Yan-yun L, Ai-ye S, Rui-yu L, A vision inspection system for the surface defects of strongly reflected metal based on multi-class SVM, Expert. Syst. Appl., 38(5), 5930-5939, 2011.
[5] Tsai DM, Huang TY, Automated surface inspection for statistical textures, Image Vision Comput., 21(4), 307-323, 2003.
[6] Tsai D, Lai S, Defect detection in periodically patterned surfaces using independent component analysis, Pattern Recognit., 41(9), 2812-2832, 2008.
[7] Li W, Tsai D, Automatic saw-mark detection in multicrystalline solar wafer images, Solar Energy Mater. Solar Cells, 95(8), 2206-2220, 2011.
[8] Lu C, Tsai D, Independent component analysis-based defect detection in patterned liquid crystal display surfaces, Image Vision Comput., 26(7), 955-970, 2008.
[9] Rosenboom L, Kreis T, Jüptner W, Surface description and defect detection by wavelet analysis, Mea. Sc. Tech., 22(4), 045102, 2011.
[10] BS EN ISO 4287:1998 Surface texture: Profile-method. Terms, definitions and surface texture parameters
[11] BS EN ISO 25178-2, Surface texture: Areal- Part 2: Terms, definitions and surface texture parameters
[12] BS EN ISO 8785:1999 Surface imperfection –terms, definitions and parameters
[13] BS EN ISO 6507-1:2005 Metallic materials: Vickers hardness test, Test method.